Journal of Applied Polymer Science

Viscoelastic and Thermal Decomposition Behaviors of Polytetrahydrofuran Binder Prepared Using Glycerin as a Crosslinking Modifier

Makoto Kohga, Tomoki Naya, Shingo Shioya
Department of Applied Chemistry, National Defense Academy, Hashirimizu 1-10-20, Yokosuka, Kanagawa 239-8686, Japan
Correspondence to: M. Kohga (E-mail: kohga@nda.ac.jp)

ABSTRACT: Polytetrahydrofuran (PTHF) is an effective binder ingredient used for improving the performance of propellants. PTHF becomes sufficiently rubbery for use as a binder with the addition of an adequate crosslinking modifier. This study investigated the viscoelastic and thermal decomposition behaviors of the PTHF binder prepared using glycerin as a crosslinking modifier, as well as the influence of the molecular weight of PTHF on the characteristics of the PTHF binder. The curing behavior of the PTHF binder was suitable for the manufacture of propellants, and the superior tensile properties of the PTHF binder made it suitable for use as a propellant binder. The degree of crosslinking of the samples decreased as the molecular weight of the PTHF increased. The PTHF binder has unique dynamic mechanical properties owing to its melting and chemical structure, and these properties were dependent on the molecular weight of PTHF. The glass transition temperature (T_g) and the loss tangent at T_g decreased as the molecular weight of the PTHF increased. The temperature and frequency dependence of the PTHF binder were influenced by the melting point of PTHF. The viscoelastic properties of the binder prepared using PTHF with a molecular weight of 650 followed the time–temperature superposition principle. The activation energy for the relaxation of this binder varied remarkably at the melting point of PTHF. The thermal decomposition behavior indicated that at low temperatures, the consumption rate of the binder with low-molecular-weight PTHF was slightly larger than that of the binder with high-molecular-weight PTHF. © 2012 Wiley Periodicals, Inc. J. Appl. Polym. Sci. 000: 000–000, 2012

KEYWORDS: viscosity and viscoelasticity; thermogravimetric analysis; swelling; mechanical properties; crosslinking

Received 16 May 2012; accepted 23 July 2012; published online
DOI: 10.1002/app.38400

INTRODUCTION

Solid propellant is commonly used as fuel for rockets and missiles. Composite propellant is a solid propellant that consists of oxidizer crystals, binder, curing agent, metal fuel, burning catalyst, and other components. The binder provides the structure or matrix in which solid granular ingredients are held together in a composite propellant. The rubbery organic binder materials also act as fuel for solid propellant rockets and are oxidized in the combustion process. The binding ingredient, which is usually some type of polymer, has a primary effect on motor reliability, mechanical properties, propellant processing complexity, storability, aging, and costs.

Composite propellant is produced by the following method. The oxidizer, binder, burning rate modifier, plasticizer, metal fuel, etc. are mixed, after which air is removed from the mixture. In the final step, the uncured propellant is cast into the case of a rocket motor and solidified in the motor case. A low-viscosity uncured propellant is desirable to enable easier mixing and casting. In addition, extending the pot life of the uncured propellant provides sufficient time for mixing and casting.

The propellant grain undergoes high stresses that are induced by rapid acceleration, sharp turns, or rapid increases in chamber pressure during launch and flying. Accordingly, it is necessary for the propellant to have mechanical properties that prevent these stresses. When the propellant grain cannot resist such stresses, cracks and defects are generated in the grains. These cracks and defects expose additional burning surfaces and thus cause an increase in the evolution of combustion gas. This can ultimately result in destruction of the motor through a sharp increase in pressure in the combustion chamber.

The development of a wide variety of rockets has required the generation of propellants having a wide range of burning performances corresponding to the purposes for which they are used. The use of propellant with a high burning rate can supply

Applied Polymer SCIENCE

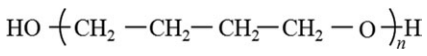

Figure 1. Chemical structure of PTHF.

a large impulse; therefore, a high burning rate propellant is needed when developing high-performance rocket motors.

According to the requirements described above, it is necessary for a composite propellant to have adequate processability, excellent mechanical properties, and favorable burning characteristics. Propellant performance is greatly dependent on the chemical and physical properties of each propellant ingredient. As mentioned above, the binder is one of the main propellant ingredients and greatly influences the propellant performance. Hydroxyl-terminated polybutadiene (HTPB) is commonly used as a binder ingredient for composite propellants because it has excellent properties for use as a propellant binder. HTPB is cured with the diisocyanates such as isophorone diisocyanate, toluene diisocyanate, and hexamethyl diisocyanate. A common diisocyanate to cure is isophorone diisocyanate (IPDI). Accordingly, the rheological properties of the HTPB binder have been examined by various researchers.[1–8]

Polytetrahydrofuran (PTHF) is used as an ingredient for rubber products. The chemical structure of PTHF is shown in Figure 1. PTHF has a linear molecular structure with a repeating unit that consists of a single bond, as well as one oxygen atom, four carbon atoms, and eight hydrogen atoms. PTHF has an OH group on one side of the molecular chain of PTHF and a hydrogen atom on the other side so that both sides of the molecular chain have a hydroxide group. Therefore, the reaction of PTHF and IPDI is the urethane reaction similar to that of HTPB and IPDI. Because is a saturated linear diol and IPDI is a diisocyanate, it cannot become a solid when only IPDI is used as the curing agent; however, it does become sufficiently rubbery for use as a binder when a triol material such as glycerin is added as a crosslinking modifier.[9]

Even though PTHF is not an energetic binder, the specific impulse and burning-rate characteristics of the composite propellant could be improved by the use of PTHF as a binder when compared to propellant prepared using HTPB because there is oxygen in the repeating unit of PTHF.[9–13] Furthermore, the processability, mechanical properties, and thermochemical behavior of the HTPB binder were improved by the addition of PTHF as a plasticizer.[14,15]

Investigation of the rheological properties and thermal decomposition behavior of a binder is necessary during the development of a propellant binder. The thermal decomposition behavior and burning characteristics of composite propellant prepared using a PTHF/glycerin system as a binder have been reported.[9,12] However, the rheological properties and thermal decomposition behavior of a PTHF/glycerin binder have not been published to date. This study was conducted to investigate the viscoelastic and thermal decomposition behaviors of a PTHF binder prepared using glycerin as a crosslinking modifier. In addition, we studied the influence of the molecular weight of PTHF on those characteristics of the PTHF binder.

EXPERIMENTAL

Sample Preparation

PTHF is produced in several different molecular weights. Three types of PTHF were used in this study: PTHF1, PTHF2, and PTHF3, which had molecular weights of 650, 1400, and 2900, respectively. The number (1, 2, or 3) suffixed to PTHF increases with increasing molecular weight. The molecular weight of PTHF2 is approximately twice that of PTHF1, and the molecular weight of PTHF3 is approximately double that of PTHF2. PTHF was supplied by DuPont. Table I shows the chemical properties of the PTHF used in this study.

IPDI (Tokyo Kasei) and glycerin (Kanto Chemical) were used as the curing agent and crosslinking modifier, respectively. Table II shows the formulations of the PTHF binders. The PTHF/IPDI/glycerin mole ratio of these systems was 1.00/1.50/0.33.[9]

PTHF was first added with glycerin, after which this mixture was sufficiently blended for $\sim$ 5 min. Glycerin is a hygroscopic material; therefore, the moisture in glycerin was removed by molecular sieves before it was added to the PTHF. Next, IPDI was added to the mixture, which was then mixed well for $\sim$ 10 min. The mixture with IPDI was maintained in a temperature-controlled oven at 353 K to cure for 1 week.[9]

Analytical Methods

We measured the viscosity of the uncured PTHF sample using a universal modular rheometer (HAAKE RheoStress 600, Thermo Electron) with a plate–plate sensor system. The diameter of the disc plate was 60 mm and the gap distance between plates was 1 mm. The shear rate was in the range of 0–1000 s^{-1}, and the temperature was 353 K.

The sample surfaces cut with a knife were examined by scanning electron microscopy (SEM; JEOL NeoScope JCM-5000). A swelling test was carried out with a rectangular parallelepiped ($20 \times 20 \times 2$ mm^3) at 298 K. Toluene was used as a swelling solvent. The mass of the sample was measured before and after immersion in toluene and the volumes were calculated. The volume fraction of the sample in the swollen sample (v_s) was determined by dividing the volume before swelling by that of the

Table I. Chemical Properties of PTHF Materials

Symbol	M_n	Density at 298 K (g cm^{-3})	Melting point (K)
PTHF1	650	0.978	284–292
PTHF2	1400	1.000	306–309
PTHF3	2900	0.970	303–316

Table II. Formulations of PTHF Binders

Binder	PTHF1 (%)	PTHF2 (%)	PTHF3 (%)	Glycerin (%)	IPDI (%)
PTHF1	64.1	–	–	3.0	32.9
PTHF2	–	79.4	–	1.7	18.9
PTHF3	–	–	88.9	0.9	10.2

Table III. Initial Viscosity of Uncured PTHF Binders at 100 s^{-1} and 353 K

Binder	Initial viscosity (Pa s)
PTHF1	0.017
PTHF2	0.625
PTHF3	0.731

swollen sample. The densities of the cured PTHF samples were in the range of 0.94–1.09 g cm^{-3}.

The tensile test was carried out using dumbbells conforming to JIS K 6251 at a crosshead speed of 500 mmmin^{-1} at 293 K with an autograph (AGS-100 A, Shimadzu). Dumbbell-shaped samples with a thickness of ~ 2 mm were punched out of the cured samples. The gage length was 20 mm. The tensile properties were determined from the average of five measurements.

The dynamic mechanical properties of the cured samples were measured using a dynamic mechanical analyzer (Tritec 2000, Triton Technology) in extension mode. The sample was a rectangular parallelepiped (6 × 3 × 20 mm^3). Both ends of the sample were mounted with clamps, and one end was held while the other end was oscillated sinusoidally at a defined frequency and displacement. The gap between the clamps was 5 mm and the displacement was 0.01 mm. The temperature dependence of the blends was measured in the temperature range of 123–353 K at a frequency of 1 Hz and a heating rate of 5 K min^{-1}. Frequency dependence was measured at intervals of 10 K in the temperature range of 233–333 K and the frequency range of 0.01–50 Hz. Under this strain condition, the material is in its linear viscoelastic region.

The thermal decompositions of the binders and propellants were measured by differential thermal analysis (DTA) and thermogravimetry (TG) using a Rigaku Thermo Plus 2 TG-DTA8120. The equipment was operated under a nitrogen flow of 0.5 dm^3 min^{-1} at atmospheric pressure. DTA and TG were carried out with a heating rate of 20 K min^{-1}.

RESULTS AND DISCUSSION

Curing Behavior

Table III shows the initial viscosities of uncured PTHF binders at 100 s^{-1} and 353 K. These PTHF binders were added with IPDI; therefore, the viscosity of the samples increased with elapsed time. As mentioned in "Sample Preparation" section, IPDI was added to the mixture of PTHF and glycerin, after which it was mixed well for ~ 10 min. The initial viscosity was measured at 10 min after IPDI was added to PTHF in this study. The initial viscosity of the uncured PTHF binder decreases with decreasing molecular weight of PTHF, and the viscosity of the PTHF1 binder was significantly smaller than those of the PTHF2 and PTHF3 binders. The HTPB binder has generally been used as a propellant binder. The initial viscosity of the HTPB binder was 0.195 Pas at 100 s^{-1} and 353 K.[16] The initial viscosity of the PTHF1 binder was approximately one-tenth that of the HTPB binder, while the viscosities of the PTHF2 and PTHF3 binders were approximately three times as large as that of the HTPB binder.

The relationships between viscosity and elapsed time for the uncured PTHF binders were not strongly dependant on the shear rate. Figure 2 shows the viscosities of the PTHF binders versus elapsed time at 100 s^{-1}. These viscosities increased with increasing time because the binders were added with IPDI as a curing agent. The increase in the viscosity of PTHF1 and PTHF2 was small until 400 min, after which it increased remarkably. After 400 min, the increasing rate of viscosity versus time for PTHF2 was slightly smaller than that for PTHF1. Conversely, the increasing rate of viscosity for PTHF3 was small until 1000 min when compared to those of the PTHF1 and PTHF2 binders.

The curing behavior of the HTPB binder is described in Ref. 16. The viscosity of the HTPB binder versus elapsed time is also shown in Figure 2. The increase in viscosity versus time of this binder was small until 30 min, after which it increased remarkably. The period from the beginning of mixing to the time at which the viscosities increased remarkably for the PTHF binders was longer than that of the HTPB binder, indicating that the pot life of the PTHF-based propellant was extended when compared to that of the HTPB-based propellant.

As described above, the initial viscosity of the PTHF1 binder was not only much smaller than those of the PTHF2 and PTHF3 binders but also approximately one-tenth that of the HTPB binder. Therefore, to ensure optimal mixing of the propellant ingredients and casting of the uncured propellant into the rocket motor case, the propellant prepared using the PTHF1 binder would be preferable to the propellant prepared using the PTHF2 and PTHF3 binders.

Morphological Analysis

The fractured surfaces of the PTHF binders were examined by SEM. The surfaces of the PTHF binders were almost identical, indicating that the surface did not depend on the molecular weight of PTHF. Figure 3 shows the typical micrograph of the surface of the PTHF2 binder. The surface was smooth without voids and cracks. The result suggested that the sample had a uniform structure.

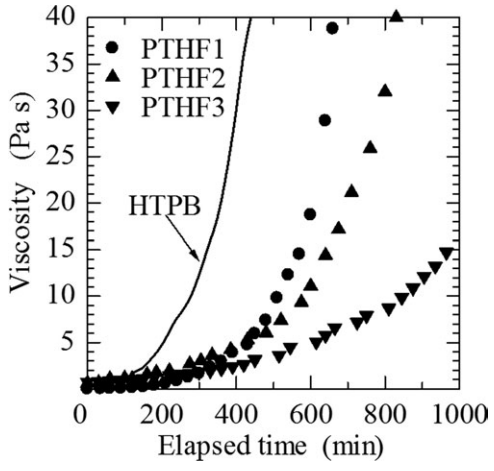

Figure 2. Relationship between viscosity and elapsed time for uncured PTHF binders at 100 s^{-1}.

Applied Polymer SCIENCE

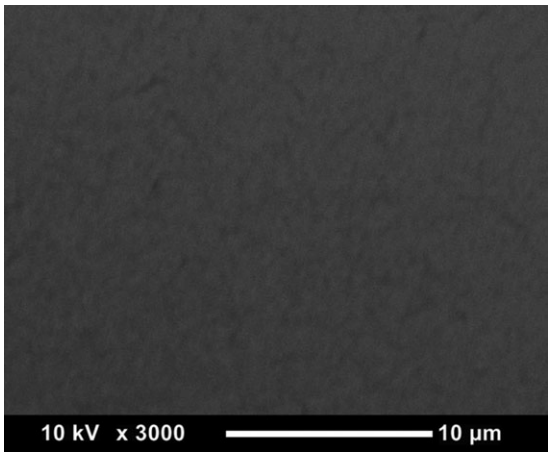

Figure 3. SEM photograph of surface of the PTHF2 binder.

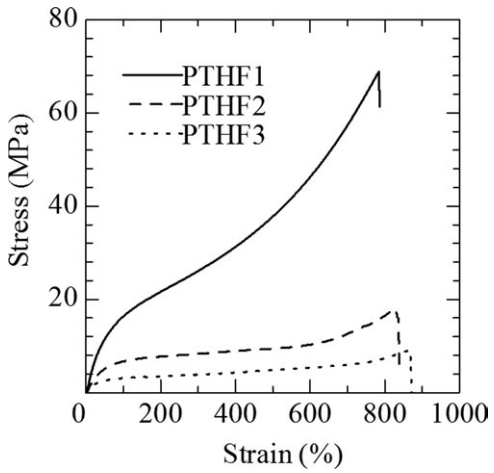

Figure 4. Stress–strain diagrams of cured PTHF binders.

Swelling Behavior

The crosslinked polymer swells with solvent to equilibrium, and the amount of swelling is dependent on the interaction between the polymer and the solvent, the length between crosslink points, the temperature, and several other factors. As mentioned in "Analytical Methods" section, v_s was determined by dividing the volume before swelling by that of the swollen sample. As the value of v_s decreases, the quantity of toluene introduced into the crosslinked polymer increases. The increase in the quantity of toluene introduced into the crosslinked polymer suggested that the degree of crosslinking (e.g., the network density) was reduced. The network density cannot be obtained from the value of v_s alone, and the polymer-solvent interaction parameter of the PTHF-toluene system is needed to calculate the network density of the cured PTHF binder.[17] However, the degree of crosslinking could be estimated with v_s.

The v_s values were calculated from the swelling experiment and are presented in Table IV. The v_s decreased as the molecular weight of PTHF increased. The value of v_s of the PTHF1 binder was approximately twice as large as that of the PTHF2 binder, while that of the PTHF2 binder was about double the v_s of the PTHF3 binder. This tendency was the same as that of the molecular weight of PTHF. These results indicated that the degree of crosslinking would decrease as the molecular weight of PTHF increases because the main chain length of PTHF increases with increasing molecular weight, which enhances the length between crosslink points.

Tensile Properties

Figure 4 shows the stress–strain diagrams obtained from the tensile test of the cured PTHF binders. The tensile stress increases with increasing tensile strain. There is an elastic region below ~ 15% of strain for these binders. The ultimate tensile strain is the same as the strain at the breaking point. The tensile strength and elongation of the cured PTHF binders are listed in Table V. The modulus was not determined because the elastic region was very narrow compared to the elongation at break. As the molecular weight of PTHF increased, the tensile strength decreased, while the elongation increased. The tensile strength between the PTHF1 and PTHF2 binders differed greatly, but that between the PTHF2 and PTHF3 binders was small, even though the molecular weight of PTHF3 was approximately twice as large as that of PTHF2.

The tensile strength generally decreases with increasing elongation because the tensile strength decreases as the network density decreases, and a lower tensile strength indicates a lower degree of crosslinking.[18] As described in "Swelling Behavior" section, the value of v_s decreased as the molecular weight of PTHF increased. In other words, the degree of crosslinking would decrease as the molecular weight of PTHF increased. The results obtained by the tensile test were consistent with the swelling behavior.

The tensile strength and elongation of the HTPB binder were 0.58 MPa and 470%, respectively.[14] The tensile strength and elongation of the PTHF binders were larger than those of the HTPB binder, indicating that PTHF samples would have superior tensile properties for the propellant binder when compared with HTPB.

Dynamic Mechanical Properties

Temperature Dependence. Figure 5 shows the temperature dependence of the modulus (E'), the loss modulus (E''), and the loss tangent for the PTHF binders. The value of E' decreased as

Table IV. Values of v_s

Binder	v_s
PTHF1	0.476
PTHF2	0.252
PTHF3	0.128

Table V. Tensile Properties of Cured PTHF Binders

Binder	Tensile strength (MPa)	Elongation (%)
PTHF1	6.89	784
PTHF2	1.80	828
PTHF3	0.91	866

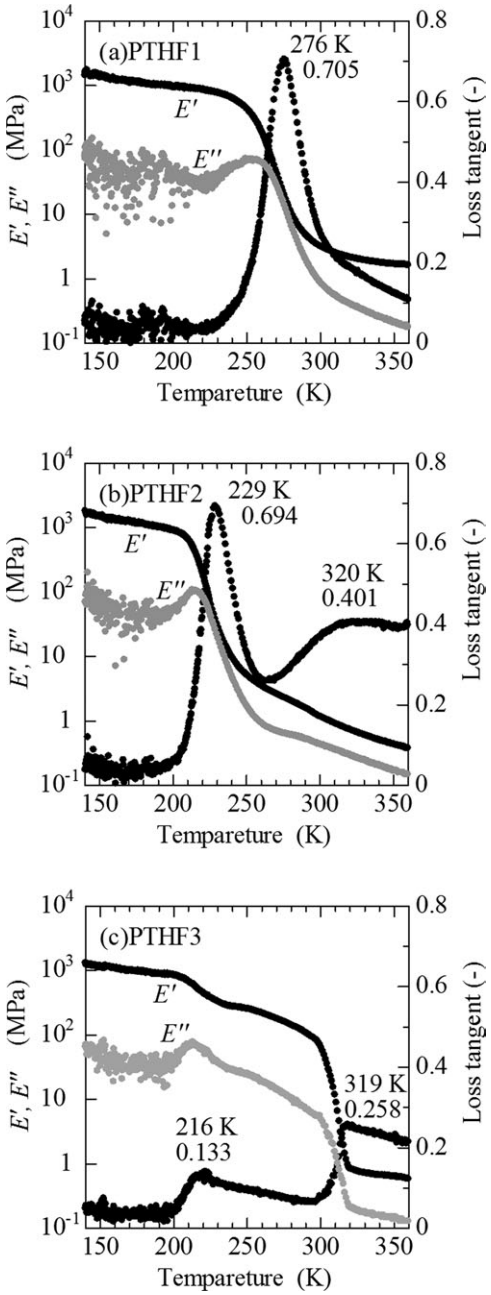

Figure 5. Temperature dependence of E', E'', and the loss tangent of the PTHF binders.

the temperature increased. The thermogram of the PTHF1 binder showed a remarkable decrease in the temperature range of 240–310 K, while that of the PTHF2 binder showed a pronounced decrease in the range of 200–250 K. The thermogram of the PTHF3 binder showed a remarkable decrease in the ranges of 200–240 K and 290–320 K, with an especially large variation being observed in the latter temperature range. The value of E'' was smaller than that of E'. The thermogram of PTHF1, PTHF2, and PTHF3 binders had a small peak at 250, 215, and 212 K, respectively. Above the peak temperature, the relationship between the temperature and E' or E'' was of the same nature.

The loss tangent of the PTHF1 binder peaked at 276 K and the loss tangent at this peak was 0.705. The thermogram of the loss tangent for the PTHF2 binder peaked at 229 K, but showed another broad peak at around 320 K. The loss tangents at these peaks were 0.694 and 0.401, respectively. The thermogram of the loss tangent for the PTHF3 binder peaked at 216 K and 319 K, and the loss tangents at the peaks were 0.133 and 0.258, respectively.

As shown in Table I, the melting point of the PTHF materials was in the range of 284–316 K. As mentioned above, the thermograms of E' and the loss tangents for the PTHF2 and PTHF3 binders varied at around 320 K, which was near the melting point of PTHF. The PTHF binders were placed in a freezer at 250 K (below the melting point of the PTHF materials) for 12 h. Figure 6 shows a photograph of the cooled PTHF binders. The PTHF binders were colorless and transparent at room temperature. Visual observation indicated that after cooling, the PTHF1 and PTHF2 binders remained colorless and transparent, while the PTHF3 binder changed from colorless and transparent to white and opaque. These findings indicated that a portion of the PTHF3 binder was crystallized below the melting point of the PTHF3 material.

The variations in the E' and loss tangent thermograms at around 320 K were likely caused by the melting of PTHF. Even when the PTHF2 and PTHF3 binders were cured and became rubbery, the melting of the PTHF material influenced the temperature dependence of these binders. The thermograms of the PTHF3 binder had especially remarkable variation at around 320 K when compared with PTHF2 owing to melting of the PTHF3. This occurred because the main chain length of PTHF3 is longer than that of PTHF2. The loss tangent thermograms of the PTHF1 binder did not have a peak at around the melting point of the PTHF1 material because the main chain length of PTHF1 is much shorter than those of PTHF2 and PTHF3. The crystalline magnitude of the PTHF binders increases with the increase in the molecular weight of PTHF.

Based on the results presented above, the peak at $\sim$ 320 K was caused by the melting of PTHF; therefore, the glass transition temperatures (T_g) of the PTHF1, PTHF2, and PTHF3 binders were 276, 229, and 216 K, respectively. The value of T_g

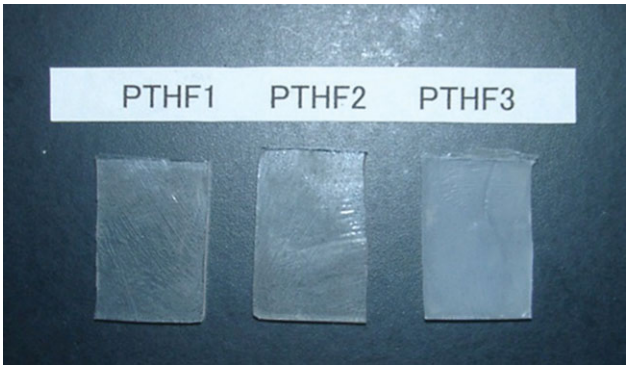

Figure 6. Photograph of the PTHF binders cooled at 250 K. [Color figure can be viewed in the online issue, which is available at wileyonlinelibrary.com.]

decreased as the molecular weight of PTHF increased. The loss tangents of PTHF1, PTHF2, and PTHF3 at T_g were 0.705, 0.694, and 0.133, respectively. The value decreased as the molecular weight of PTHF increased, and that of the PTHF3 binder was especially small when compared with the PTHF1 and PTHF2 binders.

The dynamic mechanical properties of a polymer are strongly influenced by its internal structure. The T_g decreases with the increase in the crystallinity of the polymer.[19] PTHF is a crystalline polymer and the crystalline magnitude of the PTHF binders increases with the increase in the molecular weight of PTHF as described above. Therefore, T_g decreased as the molecular weight of PTHF increased.

Furthermore, the motion of the chain segments in the polymer structure has a profound effect on T_g and the loss tangent. The values of T_g and the loss tangent are sensitive indicators of crosslinking. As the degree of crosslinking decreases, the motion of the chain segments increases, thereby decreasing T_g and increasing the loss tangent.[20,21]

The value of T_g decreased with increasing molecular weight of PTHF because the degree of crosslinking decreased as the molecular weight of PTHF increased as described in "Swelling Behavior" section. The degree of crosslinking decreased as the molecular weight of PTHF increased, suggesting that the loss tangent at T_g would increase as the molecular weight of PTHF increases. However, as described above, the value decreased as the molecular weight of PTHF increased. PTHF has a saturated linear molecular structure, and the main chain length of PTHF increases with molecular weight. The linear structure would restrict the motion of the chain segments; therefore, the loss tangent at T_g decreased with increasing molecular weight of PTHF, even though the degree of crosslinking decreased.

Frequency Dependence. Figure 7 shows the frequency dependence of E' of the PTHF binders. The value of E' increases with increasing frequency. The E' of the PTHF1 binder decreased with increasing temperature below 293 K, while above this temperature the decrease was small. For the PTHF2 binder, there was little variation in E' below 273 K and above 303 K, while the value of E' decreased with increasing temperature between 273 and 303 K. The influence of temperature on the frequency dependence of the PTHF3 binder was similar to that on the PTHF2 binder. However, the decrease in E' between 273 and 303 K was greater for the PTHF3 binder than the PTHF2 binder.

As shown in Table I, the melting point of the PTHF materials was in the range of 284–316 K. The influence of temperature on the frequency dependence of the PTHF binder was small above the melting point of the PTHF material. The frequency dependence of the PTHF1 binder was affected by the temperature below the melting point of PTHF1. Conversely, for the PTHF2 and PTHF3 binders, the influence of temperature on frequency dependence was only strong in the vicinity of the melting point.

Application of Time–Temperature Superposition Principle. A master curve at an arbitrary reference temperature is obtained by superimposing the plots of log (frequency) versus E' obtained at various temperatures. Making a master curve based on the time-temperature superposition principle is a useful method for estimation of frequency dependence in a wide range.[22] If a master curve could be obtained, the frequency dependence in a wide frequency range that cannot be measured could be predicted using data obtained in a restricted frequency range.

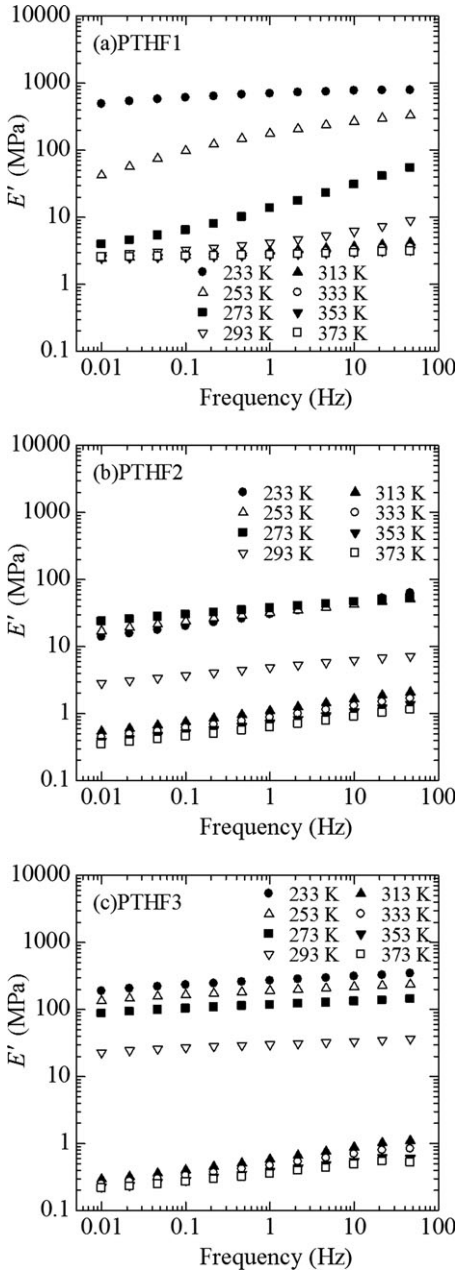

Figure 7. Frequency dependence of E' of the PTHF binders.

The plots of the PTHF1 binder fit the master curves well, while those of the PTHF2 and PTHF3 binders did not. Figure 8 shows the master curve of E' of the PTHF1 binder. The reference temperature (T_0) of the master curve was 273 K. Overall, the results revealed that the viscoelastic properties of the PTHF1 binder followed the time-temperature superposition principle.

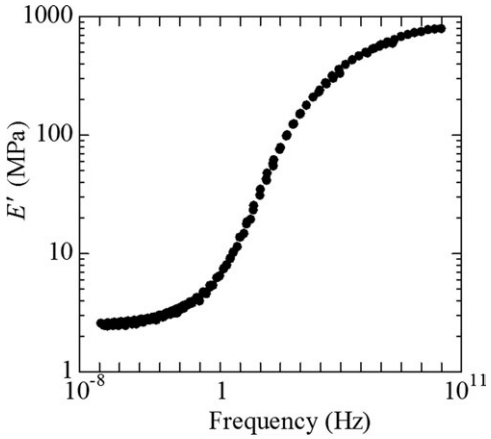

Figure 8. Master curve of E' of the PTHF1 binder.

The shift factor (α_t) represents the quantity of the shift required to superimpose the plots and is an important value needed to draw the master curve. According to the Williams–Landel–Ferry theory, α_t is expressed as[22]:

$$\log \alpha_t = -\frac{C_1(T - T_0)}{C_2 + (T - T_0)} \quad (1)$$

where T is the temperature, and C_1 and C_2 are constants. Figure 9 shows the plot of log α_t as a function of T of the PTHF1 binder. The values of log α_t are closely correlated with T. However, the values of C_1 and C_2 were not obtained to approximate this relationship. In addition, the master curve of the PTHF1 binder did not follow the Williams–Landel–Ferry approach.

According to the time-temperature superposition principle, the apparent activation energy for the relaxation (E_a) is expressed as[23]:

$$E_a = 2.303R\frac{d\log \alpha_t}{dT^{-1}} \quad (2)$$

where R is the gas constant. E_a can be calculated from the slope of the log α_t versus T^{-1} plots. Figure 10 shows the plot of log α_t as a function of T^{-1} of the PTHF1 binder. The relationship between log α_t and T^{-1} is divided into two regions and the critical point is at $T^{-1} = 0.00334$ K^{-1}, i.e., $T = 299$ K. The plots in each temperature region are described by a straight line. The relaxation mechanism of this binder would vary at around 299 K. The E_a in each temperature region was calculated from Figure 10. The value of E_a was 221 kJmol^{-1} below 299 K and 52 kJmol^{-1} above 299 K. The E_a above 299 K was approximately one-fourth of that below 299 K.

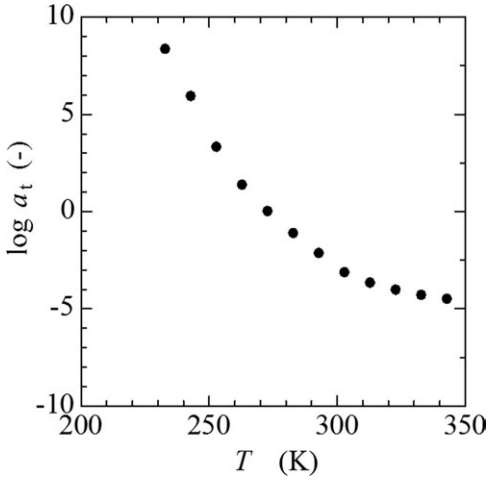

Figure 9. log α_t as a function of T of the PTHF1 binder.

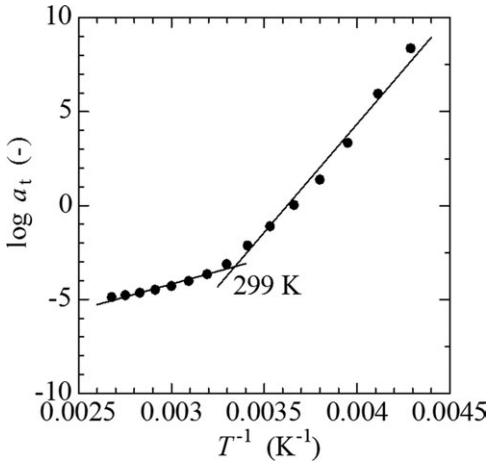

Figure 10. log α_t as a function of T^{-1} of the PTHF1 binder.

The critical point obtained in Figure 10 almost agreed with the melting point of PTHF1. The relaxation mechanism of the PTHF1 binder was varied at 299 K, which was near the melting point of the PTHF1 material. The value of E_a above 299 K was much smaller than that below 299 K because the PTHF1 material that comprised the binder became very flexible above the melting point.

As described in "Temperature Dependence" section, the influence of the melting point of PTHF1 on the temperature dependence of the PTHF1 binder was not detected. However, the relaxation of the PTHF1 binder was affected by the melting point of PTHF1; therefore, E_a varied remarkably at the melting point.

Thermal Decomposition Behavior

The burning process of the composite propellant begins with the decomposition gases of propellant ingredients being produced at the burning surface by heating. These gases diffuse and mix in the gas phase and finally burn. Accordingly, the thermal decomposition behavior of the propellant binder influences the burning characteristics of the propellant. TG-DTA is a popular method for investigation of the thermal decomposition behavior of materials and has been used to investigate several types of binders.[24–27]

The TG-DTA curves of the PTHF2 binder are provided in Ref. 12. The thermal decomposition behavior of PTHF binders prepared with different molecular weights of PTHF was investigated by TG-DTA, and the effects of the molecular weight of PTHF on the thermal decomposition behavior of the PTHF binders are described in this section. The TG-DTA measurements were conducted more than four times for each

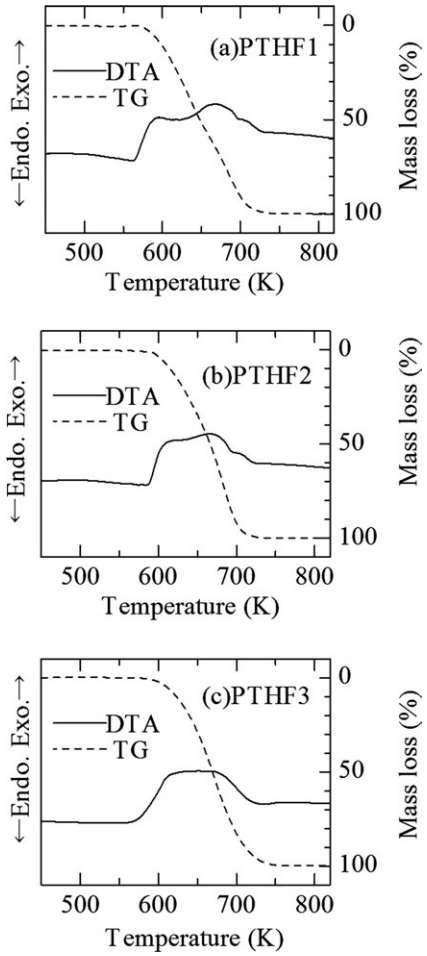

Figure 11. TG-DTA curves of PTHF binders.

sample. The experimental results revealed very good accuracy and reproducibility.

Figure 11 shows the TG-DTA curves of the PTHF binders. Based on the DTA curves, the exothermic decomposition occurs in the range of 570–720 K and a definitive peak is not observed in the DTA curve. According to the TG curves, the consumption begins at ~ 580 K, and the sample is completely consumed at around 730 K.

The consumption rate of the PTHF binders was determined from the first-derivative mass loss. Figure 12 shows the first-derivative mass loss curves of the PTHF binders. The first-derivative curve of the PTHF1 binder has two peaks at 635 and 680 K, whereas those of the PTHF2 and PTHF3 binders have one at ~ 675 K. Thus, the PTHF1 binder decomposed at a lower temperature than the PTHF2 and PTHF3 binders.

During thermal decomposition of polymer, various bonds in the polymer rupture, which results in the production of smaller fragments being produced. Above 530 K, sufficient energy becomes available for the scission of the strong chemical bonds, resulting in the generation of volatile products.[28,29]

The consumption of the PTHF binders occurred above 580 K. The PTHF binders showed peaks in the range of 673–680 K, and these peaks were very large. These findings suggest that the consumption in this temperature range would be a result of scission of the main chain of PTHF. The first-derivative curve of the PTHF1 binder had a definitive peak at 635 K, while those of the PTHF2 and PTHF3 binders did not. The value of the first-derivative mass loss at 635 K decreased with increasing molecular weight of PTHF. As described above, the degree of crosslinking of the PTHF binder decreased as the molecular weight of PTHF decreased. The consumption at around 635 K was likely caused by scission around the crosslink point.

For composite propellants, the decomposition gases of the oxidizer and binder diffuse to the gas phase and burn afterward. Decomposition at low temperatures indicates that the decomposition gases can be emitted from the propellant surface at low

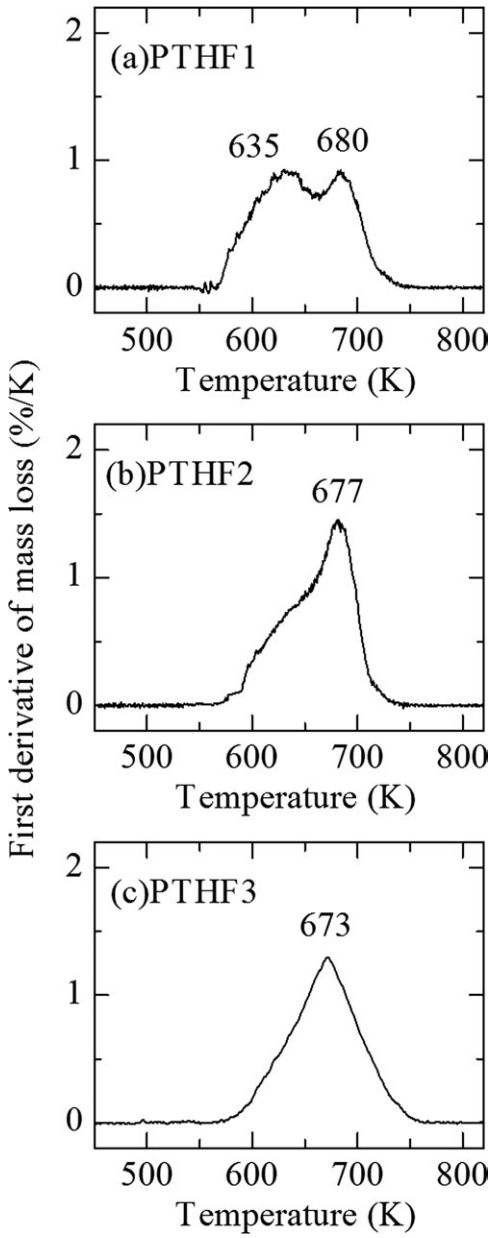

Figure 12. First derivative mass loss curves of PTHF binders.

temperatures. This suggests that it could be possible to improve the combustion of the propellant decomposition gases, and that the burning rate could increase.

As described above, the PTHF1 binder decomposed at a lower temperature than the PTHF2 and PTHF3 binders. The thermal decomposition behavior of the PTHF1 binder is preferable for obtaining a propellant with a high burning rate.

CONCLUSIONS

The objective of this study was to investigate the rheological properties and thermal decomposition behavior of a polytetrahydrofuran (PTHF) binder prepared using glycerin as a crosslinking modifier and to clarify the influence of the molecular weight of PTHF on the characteristics of PTHF binders. The initial viscosity of the uncured PTHF binder was found to decrease with decreasing molecular weight of PTHF. For the PTHF binder with high molecular weight, the rate of increase in viscosity versus elapsed time was small. As the molecular weight of PTHF increased, the tensile strength of the PTHF binders decreased, while the elongation increased. The curing behavior of the PTHF binder was suitable for the manufacture of propellants, and the superior tensile properties of the PTHF binder made it suitable for use as a propellant binder.

The swelling experiment revealed that the degree of crosslinking of the cured binder would decrease with the increase in the molecular weight of PTHF. The glass transition temperature (T_g) and the loss tangent at T_g decreased as the molecular weight of PTHF increased. The variation of the temperature dependence around the melting point of PTHF increased with the increase in the molecular weight of PTHF. The frequency dependence was small above the melting point of PTHF. The viscoelastic properties of the binder, prepared using PTHF with a molecular weight of 650, followed the time–temperature superposition principle. The activation energy for the relaxation of this binder varied remarkably at the melting point of PTHF.

The thermal decomposition behavior indicated that at low temperatures, the consumption rate of the binder with low-molecular-weight PTHF was slightly larger than that of the binder with high-molecular-weight PTHF.

Investigation of crosslinking modifiers for the PTHF binder is necessary to obtain a propellant binder with more favorable rheological properties and thermal decomposition behavior.

REFERENCES

1. Sekkar, V.; Devi, K. A.; Ninan, K. N. *J. Appl. Polym. Sci.* **2001, 79, 1869.**
2. Bandgar, B. M.; Krishnamurthy, V. N.; Mukundan, T.; Sharma, K. C. *J. Appl. Polym. Sci.* **2002,** *85*, 1002.
3. De La Fuente, J. L.; Fernández-García, M.; Cerrada, M. L. *J. Appl. Polym. Sci.* **2003,** *88*, 1705.
4. Subramanian, K.; Sastri, K. S. *J. Appl. Polym. Sci.* **2003,** *90*, 2813.
5. Gulmus, S. A.; Yilmazer, U. *J. Appl. Polym. Sci.* **2005,** *98*, 439.
6. Seifolazadeh, A.; Edrissi, M. *Intern. J. Eng. B* **2005,** *18*, 413.
7. Reddy, T. S.; Nair, J. K.; Satpute, R. S.; Wagh, R. M.; Sikder, A. K.; Venugopalan, S. *J. Appl. Polym. Sci.* **2007, 106, 1885.**
8. Kohga, M. *J. Appl. Polym. Sci.* **2011,** *122*, 706.
9. Kohga, M.; Miyano, W.; Kojima, T. *J. Propul. Power* **2006,** *22*, 1418.
10. Goleniewski, J. R.; Roberts, J. A. US Patent 5,783,769, **1998.**
11. Anderson, R. C.; Zisette, C. B.; Ciccarelli, R. D.; Cragun, R. B.; Crilly, M. G.; Delaney, J. E. US Patent 6,484,617, **2002.**
12. Kohga, M.; Okamoto, K. *Combust. Flame* **2011,** *158*, 573.
13. Okamoto, K.; Kohga, M. *Sci. Technol. Energ. Mater.* **2009,** *70*, 87.
14. Kohga, M. *Sci. Technol. Energ. Mater.* **2010,** *71*, 77.
15. Kohga, M. *Sci. Technol. Energ. Mater.* **2010,** *71*, 145.
16. Kohga, M.; Hagihara, Y. *Kayaku Gakkaishi (Sci. Technol. Energ. Mater.)* **1998,** *59*, 1.
17. Rodriguez, F. Principles of Polymer Systems; McGraw-Hill: London, **1984;** p 23.
18. Billmeyer, F. W. Textbook of Polymer Science, 3rd ed.; Wiley: New York, **1984;** p 246.
19. Sperling, L. H. Introduction to Physical Polymer Science, 2nd ed.; Wiley: New York, **1992;** p 360.
20. Murakami, K. Yasashii Reologii; Sangyo Tosho: Tokyo, **2002;** p 126.
21. Murayama, T. Material Science Monographs—Dynamic Mechanical Analysis of Polymeric Material; Elsevier Scientific Publishing Company: New York, **1978;** Vol. 1, p 86.
22. Tanner, R. I. Engineering Rheology; Oxford University Press: New York, **1988;** p 351.
23. Sperling, L. H. Introduction to Physical Polymer Science, 2nd ed.; Wiley: New York, **1992;** p 345.
24. Kohga, M.; Hagihara, Y. *Sci. Technol. Energ. Mater.* **2003,** *64*, 75.
25. Kohga, M.; Hagihara, Y. *Sci. Technol. Energ. Mater.* **2003,** *64*, 110.
26. Rocco, J. A. F. F.; Lima, J. E. S.; Frutuoso, A. G.; Iha, K.; Inashiro, M.; Matos, J. R.; Suarez-Iha, M. E. V. *J. Therm. Anal. Cal.* **2004,** *75*, 551.
27. Rocco, J. A. F. F.; Lima, J. E. S.; Frutuoso, A. G.; Iha, K.; Inashiro, M.; Matos, J. R.; Suarez-Iha, M. E. V. *J. Therm. Anal. Cal.* **2004,** *77*, 803.
28. Geuskens, G. Degradation and Stabilization of Polymers; Applied Science Publishers: London, **1975;** p 15.
29. Kishre, K.; Nagarajan, R. *J. Polym. Eng.* **1987,** *7*, 319.